Evidence for a $Z < 8$ Origin of the Source Subtracted Near Infrared Background

Rodger I. Thompson, Daniel Eisenstein, Xiaohui Fan and Marcia Rieke

Steward Observatory, University of Arizona, Tucson, AZ 85721

rthompson@as.arizona.edu, deisenstein@as.arizona.edu, fan@as.arizona.edu, mrieke@as.arizona.edu

Robert C. Kennicutt[1]

Institute of Astronomy, University of Cambridge, Cambridge CB3 OHA UK

robk@ast.cam.ac.uk

ABSTRACT

This letter extends our previous fluctuation analysis of the near infrared background at 1.6μm to the 1.1μm (F110W) image of the Hubble Ultra Deep field. When all detectable sources are removed the ratio of fluctuation power in the two images is consistent with the ratio expected for faint, $z < 8$, sources, and is inconsistent with the expected ratio for galaxies with $z > 8$. We also use numerically redshifted model galaxy spectral energy distributions for 50 and 10 million year old galaxies to predict the expected fluctuation power at 3.6μm and 4.5μm to compare with recent *Spitzer* observations. The predicted fluctuation power for galaxies at z = 0–12 matches the observed *Spitzer* fluctuation power while the predicted power for $z > 13$ galaxies is much higher than the observed values. As was found in the 1.6μm (F160W) analysis the fluctuation power in the source subtracted F110W image is two orders of magnitude below the power in the image with all sources present. This leads to the conclusion that the 0.8–1.8μm near infrared background is due to resolved galaxies in the redshift range $z < 8$, with the majority of power in the redshift range of 0.5–1.5.

Subject headings: cosmology: observations – diffuse radiation – early universe, galaxies: high-redshift

---

[1]Steward Observatory, University of Arizona, Tucson, AZ 85721

1. Introduction

In a previous paper (Thompson et al. 2007) we addressed the nature of the Near InfraRed Background (NIRB) at 1.6μm using NICMOS observations in the Hubble Ultra Deep Field (HUDF). The area covered by the NICMOS observations comprises the NICMOS Ultra Deep Field (NUDF) which is smaller than the HUDF. The NIRB at 1.1μm and 1.6μm has a total power of 7 nWm^{-2}sr^{-1} emitted by resolved galaxies, predominantly in the redshift range z = 0.5–1.5. This is in contrast to the previous results from Matsumoto et al. (2005) that claimed a peak flux of 70 nWm^{-2}sr^{-1} at 1.4μm. The discrepancy arose not in the value of the total measured flux but in the attribution of the flux to the components of zodiacal emission, resolved stars and galaxies and an excess. In Matsumoto et al. (2005) models were used to determine the first two components and the difference between the modeled components and the total observed flux was attributed to an excess. The Matsumoto et al. (2005) measurements did not extend shortward of 1.4μm and the sharp drop in the flux levels between the 1.4μm value and shorter wavelengths was initially attributed by some authors (eg. Salvaterra & Ferrara (2003)) as due to the Lyman break in very high redshift galaxies. Our analysis measured the flux from the resolved stars and galaxies and the zodiacal background and found no excess. The difference was in the amount of flux attributed to the zodiacal background. Our measured value was higher than the modeled value used by Matsumoto et al. (2005) and the difference was equal to the flux attributed to an excess. We therefore concluded that unless there was a extragalactic flux component that was extremely flat, mimicking zodiacal flux, there is no excess and the near infrared background is resolved.

Thompson et al. (2007) also addressed the spatial fluctuations in the NUDF field relative to the fluctuations found in deep calibration 2MASS images at the same wavelength by Kashlinsky et al. (2002). Kashlinsky et al. (2002) subtracted all of the resolved sources from the 2MASS images and found fluctuations in excess of that expected by shot noise at long wavelengths. The excess was attributed to fluctuation power from galaxies at redshifts of 10 and above in several studies (eg. Magliocchetti, Salvaterra & Ferrara (2003)). A fluctuation analysis of the NUDF F160W image showed that when sources were removed from the NICMOS image down to the level that were removed from the 2MASS image, the fluctuations were consistent with those found by Kashlinsky et al. (2002). When sources were removed down to the detection limit of the combined ACS and NICMOS observations in the NUDF the fluctuation power dropped by almost two orders of magnitude. Since all of the detected sources had redshifts between 0 and 8, this meant that the fluctuations found by Kashlinsky et al. (2002) were from galaxies in the redshift range between 0 and 8. Further analysis in Thompson et al. (2007) of images that only retained sources in a given redshift bin determined that the majority of fluctuation power came from galaxies in redshift range between 0.5 and 1.5. The fluctuation spectra from galaxies with redshifts greater than 4

were not detectable above the noise.

More recent fluctuation analyses of *Spitzer* IRAC images at 3.6μm and 4.5μm (Kashlinsky et al. (2005) and Kashlinsky et al. (2007b)) interpret the residual fluctuations after source subtraction as being due to high redshift, possibly Population III, galaxies (Kashlinsky et al. 2007a). This assertion appears to be based on the assumption that all galaxies below the IRAC detection limit must be faint due to their high redshift. This interpretation has been challenged by Cooray et al. (2007) who did further source subtraction in the field using deep ACS images to identify faint sources missed by the IRAC images. They found the removal of these sources greatly reduced the signal seen by Kashlinsky et al. (2007b) and the signal must be due to sources with redshifts less than 8 that are visible in the ACS images. Kashlinsky et al. (2007a) replied that the excessive amount of area removed from the IRAC images in the source subtraction carried out by Cooray et al. (2007) invalidates their result. Modeling by Salvaterra et al. (2006) indicates that the observed IRAC fluctuations may be consistent with those created by Pop II stars at redshift greater than or equal to 5. The present study is motivated in part by a desire to investigate whether the observations in the NUDF at both 1.1μm and 1.6μm are consistent with the high redshift interpretation of the the IRAC observations by examining the color of the fluctuations and their expected extrapolation to the IRAC bands.

2.   Data and Analysis

The location, size and pixel scale of the F110W image is identical to the F160W NUDF image analyzed in Thompson et al. (2007). Details of the image preparation are given in Thompson et al. (2005). The basic image production after the processing of the individual images is production of a background image which is the median of all of the individual images, subtraction of the background from the individual images and then combining the images with the drizzle procedure (Fruchter and Hook 2002). The fluctuation analysis of the F110W image is identical to the analysis techniques used on the F160W image in Thompson et al. (2007) and is not repeated in detail here. Source subtraction is accomplished using the SExtractor (Bertin and Arnout 1996) (SE) pixel map where each pixel that is part of a source is given a value equal to the source ID number and all other pixels have a value of zero. The photometric redshifts derived in Thompson et al. (2006) were used to identify the redshift of each source. Due to the much higher resolution of the NICMOS images relative to the IRAC images, even the all source subtracted image retained 93% of its pixels. This means that the objections of Kashlinsky et al. (2007a) to the Cooray et al. (2007) analysis do not apply here. All source pixels were set to zero in the subtracted image.

There was no attempt to replace them with random noise. The small area of the subtracted sources means that this had no affect on the final fluctuation spectrum. Figure 1 shows the fluctuation power at 1.1μm and 1.6μm. To determine the redshift distribution of the 1.1μm fluctuations the fluctuation analysis was also performed on the 1.1μm image with all sources except those in a given redshift bin removed. The 1.1μm fluctuation power versus redshift distribution is essentially identical to the 1.6μm distribution shown in Figure 6 of Thompson et al. (2007). There is a peak near z=1 and no discernible power above the background for $z > 4$.

3. Fluctuation Colors

To investigate the nature of the sources of the fluctuation power observed in the all source subtracted NICMOS and IRAC images we calculate the expected fluctuation power color as a function of redshift using galaxy Spectral Energy Distributions (SEDs). At any given angular scale the fluctuation power for a given wavelength band is directly proportional to the power of the galaxies (νI_ν) in that band. The power ratios of the bands at any redshift are easily calculated from the numerically redshifted model SEDs. The analysis of Thompson et al. (2006) used 7 primary template SEDs labeled 1–7 going from early to late galaxies. The first 5 are observed SEDs and SEDs 6 and 7 are calculated from the models of Bruzual & Charlot (2003). The properties of these models are given in Table 1. Template 6 is for a 50 million year old galaxy and Template 7 is for a 10 million year old galaxy with the lowest metallicity available in the Bruzual & Charlot (2003) models. Template 7 is similar to a Pop. III SED but redder than a true Pop. III SED (see Schaerer (2002) for the expected differences). Although a Pop. III SED may be bluer than template 7, the sharp increase in the 3.6μm to 1.6μm fluctuation power at high redshift is due to the Lyman break passing through the 1.6μm and is therefore relatively independent of the SED to the red of the break.

Thompson et al. (2006) interpolated between the SEDs in increments of 0.1 to produce a final set of 61 different model SEDs. Figure 2 shows the distribution of the template numbers for all sources in the NUDF with redshifts greater than 2.0. The predominance of sources concentrate on templates 6 and 7, therefore, we will take them as the most probable SEDs for sources fainter than our source detection limit. We use these SEDs and the effective response functions in the NICMOS and IRAC filters to calculate the expected ratios of the power at redshifts between 0 and 15. Absorption in the Inter-Galactic Medium is modeled according to the treatment given in Madau et al. (1996).

The horizontal lines in Figure 3 show the observed ratios of the fluctuation power in the all source subtracted images using; this analysis, Kashlinsky et al. (2007b) and Thompson et al.

(2007). Since the excess fluctuation power attributed to high redshift galaxies by Kashlinsky et al. (2007b) is at angular scales greater than $30''$ the horizontal lines show the ratios observed at $100''$, the largest NICMOS angular scale.

The observed 1.1μm to 1.6μm fluctuation power ratio is consistent with the lower redshift template 6 predictions, but is incompatible with the calculated ratios at $z > 8$ for either of the templates. This is strong evidence that the source subtracted fluctuations in the NICMOS images are due to galaxies at $z < 8$. The observed 3.6μm to 1.6μm ratio lies between the ratios predicted by templates 6 and 7. Given the good match to the NICMOS flux ratios for template 6 we would expect higher 3.6μm fluctuations than observed. The difference may be due to cosmic variance since the fields are different. It may also be that the much broader *Spitzer* PSFs subtract more background flux than the HST PSFs. For $z > 12$ the predicted ratios become incompatible with observations. The 4.5μm to 3.6μm ratio is essentially independent of redshift at the redshifts considered and therefore does not contribute any information on the redshift epoch of the fluctuations. The apparent agreement between the predicted and observed ratios for those bands, however, is further evidence that the observed fluctuations are due to faint galaxies at redshifts less than 8.

3.1. Compatibility of the Data Sets

An important question when comparing the NICMOS and IRAC source subtracted remnant fluctuations is whether sources are subtracted to the same level in both data sets. Although Kashlinsky et al. (2007b) does not explicitly state the achieved source subtraction level, Kashlinsky et al. (2007a) states that any remaining sources in the IRAC image must be fainter than 10–20 nJy. For the SEDs used in this study the IRAC limit corresponds to a NICMOS limit of 4.5–9 nJy. From Figure 3b from Thompson et al. (2007) the completeness limit is approximately 20 nJy at 1.6μm, which is 2 to 4 times brighter than the IRAC subtraction limit. The sources for subtraction, however, were identified using detections in a combination of the ACS and NICMOS HUDF images, with the ACS images going significantly deeper due to their much longer integration time. Figure 7 in Thompson et al. (2006) shows that the detection limit in the ACS F775W band is approximately 30 in AB magnitudes which is 3.7 nJy. We can use the SEDs discussed in §3 to see what IRAC fluxes these correspond to. The results are shown Figure 4. Template SED 6 gives a limit of 20 nJy and the bluer template 7 SED gives a limit of 10 nJy which are compatible with the IRAC subtraction limits given by Kashlinsky et al. (2007a). The F775W band only removes sources at that limit for redshifts less than 3 but the ACS F850LP long pass filter removes sources at that limit for redshifts up to 6. The two data sets are compatible for all redshifts less than

6. At redshifts between 6 and 8 the NICMOS subtraction limit is not as stringent as the IRAC subtraction limit. To account for this difference the horizontal solid line in Figures 3a and b would have to be raised by a factor of 2 to 4 but that would still not be compatible with redshifts greater than 12. The redshift distribution of galaxies with NICMOS fluxes less than 20 nJy would have to be significantly different than galaxies above this limit for the z = 6–8 sources to contribute any power to the observed NICMOS fluctuations.

3.2. Signal or Noise?

All of the discussion above is predicated on the assumption that the fluctuations observed after source subtraction are due to faint galaxies below the detection limit and not noise sources from the instrument or telescope. To check for the signature of Gaussian distributed noise in the NICMOS images we populated an image of the same size as the UDF F110W and F160W images with random Gaussian distributed noise with a variance equal to that found in the real images. An identical fluctuation analysis gives the results shown by the triangles in Figure 1. The random noise is close to the observed fluctuation power at small angular scales, but is far below the observed power at angular scales of $10''$ and larger, the region considered in this analysis. We therefore conclude that the observed fluctuation power is not due to random noise components such as read noise, Poisson photon statistics, or dark current in the NICMOS images.

We originally did not include the F110W image in the fluctuation analysis due to the possibility of residual flat fielding errors. The median of the 144 individual images measures any flat field errors very accurately. The F110W mosaic image created by replacing all of the individual actual images with the median image does appear to contain a component of noise due to small flat field errors. It is evident as the higher fluctuation power in Figure 1a at spatial scales between $10''$ and $80''$. A similar signature is not present in the 1.1μm source subtracted fluctuation power. This indicates that the subtraction of the median image from each actual image before the mosaic accurately removes any flat field errors in the regions that have no detectable sources. These are the regions that contribute to the all source subtracted fluctuation power. We therefore exclude flat fielding errors as a source of fluctuation power.

If the source subtracted fluctuations are due to faint, low redshift, galaxies then the 1.1μm and 1.6μm source subtracted images should be spatially correlated. A simple check for correlation is to subtract the F110W image from the F160W to test whether the fluctuations are reduced as would be expected if they are correlated. Since the exact scaling is not known we subtracted the F110W image with scalings between 0 and 2 in 0.1 increments. The log weighted sum of the fluctuation powers for angular scales greater than $30''$ versus the scale

factor is shown in Figure 5a. There is a broad minimum for a scale factor of 0.6, near the observed ratio of F160W to F110W fluctuation of 0.75 at $100''$. Figure 5b shows the nested fluctuation spectra. This shows that the subtraction of the scaled F110W image reduces and alters the fluctuation spectrum at larger angular scales. It also indicates that the two images are partially correlated after the subtraction of all known sources as would be expected if fainter undetected sources were present in the images. The lower boundary in Figure 5b is the upper limit on fluctuation power contributed by high redshift, 1.1μm dropout, galaxies plus any remaining noise in the images. This limit is still above the Gaussian noise spectrum shown in Figure 1a and b.

At the largest scale of $100''$ the residual fluctuation power in the F160W minus F110W image is 0.2 nWm^{-2}sr^{-1}. If the residual is due to sources with redshifts less than 10 then the expected power in the IRAC 3.6μm band is 0.02–0.2 nWm^{-2}sr^{-1} depending on which SED template is used. This is consistent with the 0.1 nWm^{-2}sr^{-1} power observed by Kashlinsky et al. (2007b) at the same spatial scale. If the residual power is due to galaxies at redshifts greater than 8 then the predicted power is in the range of 0.04 to a very large number depending on the SED and redshift. The predicted power starts to exceed the observed flux at a redshift of 11 for template 6 and at a redshift of 12 for template 7. At a redshift of 13.5 the predicted power exceeds the observed 3.6μm power by a factor of 10 for both SEDs. The residual F160W minus F110W power to 3.6μm power ratio is therefore consistent with emission from galaxies with redshifts less than 8 but cannot definitively rule out that the observed 3.6μm fluctuation power comes from galaxies in the redshift range between 8 and 13. Redshifts beyond 13, however, are not consistent with the ratio if the difference between the lower limit in Figure 5b and the Gaussian noise is due to real sources. It should be noted, however, that the predominant source of fluctuation power in the observed sources comes from galaxies at redshifts between 0.5 and 1.5. Having the residual F160W minus F110W fluctuation power coming from galaxies with redshifts above 8 would require a remarkable suppression of the luminosity function of the 0.5–1.5 redshift galaxies at low luminosities.

A final, but not as compelling, piece of evidence that the residual fluctuations are due to galaxies is that the 1.1μm to 1.6μm fluctuation power color is similar to that expected from $z < 8$ galaxies. We cannot completely rule out an unknown source of spatial power, which would be the same in both images due to their similar observation pattern and data analysis. However, in the absence of any known source of such spatial power we conclude that the NICMOS source subtracted fluctuations are due to faint, $z < 8$, galaxies below the detection limit. These galaxies become evident in the fluctuation analysis because it utilizes 93% of the pixels while the detected source power is contributed by only 7% of the image pixels.

Without far more knowledge of the IRAC instrument and data analysis procedures than we currently possess we cannot make the same arguments for the faint galaxy origin of the IRAC fluctuations. We can say that the IRAC fluctuations are at the levels predicted for faint, $z < 8$, galaxies from the NICMOS observations. Since all four bands have ratios consistent with a faint, $z < 8$, galaxies origin we assume that the fluctuations in all four bands have extragalactic origins. We note that even if the IRAC fluctuations were due to noise, it would still support our conclusions that the IRAC fluctuations are not due to very high redshift galaxies.

4. Conclusions

Our basic conclusion is that the source subtracted fluctuations observed in the two NICMOS bands and the IRAC bands at 3.6μm and 4.5μm are consistent with faint, $z < 8$, galaxies that are below the individual detection limit in the respective images. We also conclude that the observed ratio of 1.1μm to 1.6μm fluctuations is incompatible with a significant fraction of power from $z > 8$ galaxies and that the ratio of the IRAC 3.6μm to NICMOS 1.6μm fluctuation power is incompatible for galaxies at $z > 13$. In light of these observations we find no evidence that any of the observed fluctuations require flux from high redshift galaxies. Of course such galaxies may exist, but we conclude that they do not contribute measurable power to the current observations.

The argument in Kashlinsky et al. (2007a) for the IRAC fluctuations being due to high redshift galaxies appears to be based on the assumption that any sources fainter than their detection limit must be at high redshift because they are faint. Examination of Figure 3b in Thompson et al. (2007) shows that the z = 0–7 galaxy luminosity function shows no break up to a completeness limit of 5 nJy in the F160W band. This implies that there are many more low redshift galaxies fainter than the detection limit, i.e. galaxies that are not faint because they are at $z > 8$.

A caveat relevant to this study is that if it is postulated that the IRAC fluctuations are due to galaxies with $z > 13$ then the predicted 1.6μm fluctuations would be below our detection level due to the very high ratio of IRAC power to NICMOS power at high redshifts. However if these high-redshift galaxies are the only source of the IRAC fluctuations, then a mechanism must be found to suppress the low redshift IRAC fluctuations predicted from the NICMOS residual fluctuations. At this time we know of no such mechanism.

REFERENCES

Bertin, E., and Arnouts, S. 1996, A&A, 117, 393.

Bruzual, G. & Charlot, S., 2003, MNRAS, 344, 1000

Chabrier, G. 2003, PASP, 115, 763

Cooray, A., et al. 2007, ApJ, 659, L91

Fruchter, A.S. & Hook, R.N. 2002, PASP, 114, 144.

Kashlinsky, A. et al. 2002, ApJ, 579, L53

Kashlinsky, A., Arendt, R. G., Mather, J., & Mosley, S. H. 2005, Nature, 438, 45

Kashlinsky, A. 2007, astro-ph/0701147

Kashlinsky, A., Arendt, R.G., Mather, J. & Moseley, S.H. 2007, ApJ, 654, L1, (Kashlinsky et al. 2007a)

Kashlinsky, A., Arendt, R.G., Mather, J. & Moseley, S.H. 2007, ApJ, 654, L5, (Kashlinsky et al. 2007b).

Madau, P., Ferguson, H.C., Dickinson, M. E.,Giavalisco, M., Steidel, C. C. & Fruchter, A. 1996, MNRAS, 283, 1388.

Magliocchetti, M., Salvaterra, R., & Ferrara, A. 2003, MNRAS, 342, L25

Matsumoto, T. et al. 2005, ApJ, 626, 31

Salvaterra, R., Ferrara, A. 2003, MNRAS, 339, 973

Salvaterra, R., Magliocchetti, M., Ferrara, A & Schneider, R. 2006, MNRAS, 368, L6.

Schaerer, D. 2002, A&A, 382, 28.

Thompson, R. I., et al. AJ, 130, 1

Thompson, R. I. 2006, ApJ, 647, 787

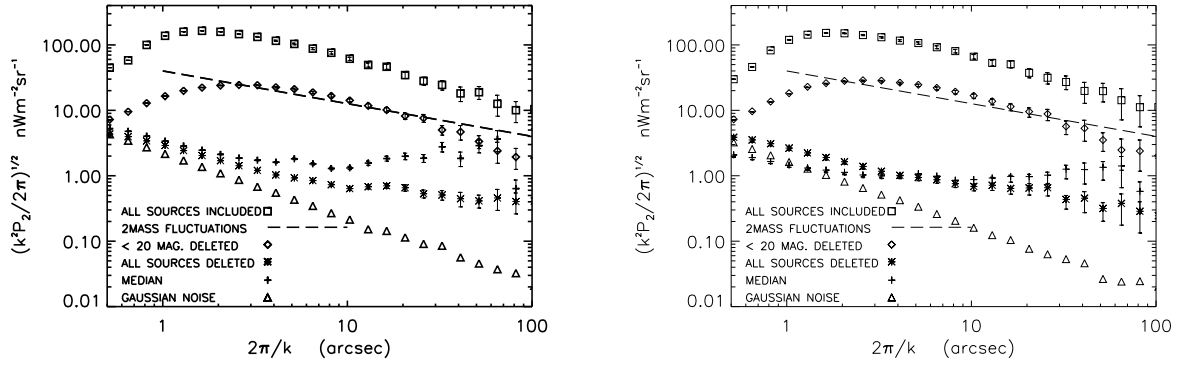Thompson, R.I., Eisenstein, D., Fan, X., Rieke, M., & Kennicutt, R.K. 2007, ApJ, 657, 669.

Fig. 1.— The fluctuation spectra from a) the F110W NUDF image (left) and b) the F160W image (right). The open squares are for no sources subtracted, the open diamonds are for all sources with a F160W AB magnitude of 20 or brighter subtracted. The asterisks are for all sources subtracted and the crosses are for the median background field described in the text. The open triangles are for a Gaussian distributed noise image with a standard deviation equal to that of the images. The dashed line indicates the level of 1.6μm fluctuations found in deep calibration 2MASS fields by Kashlinsky et al. (2002).
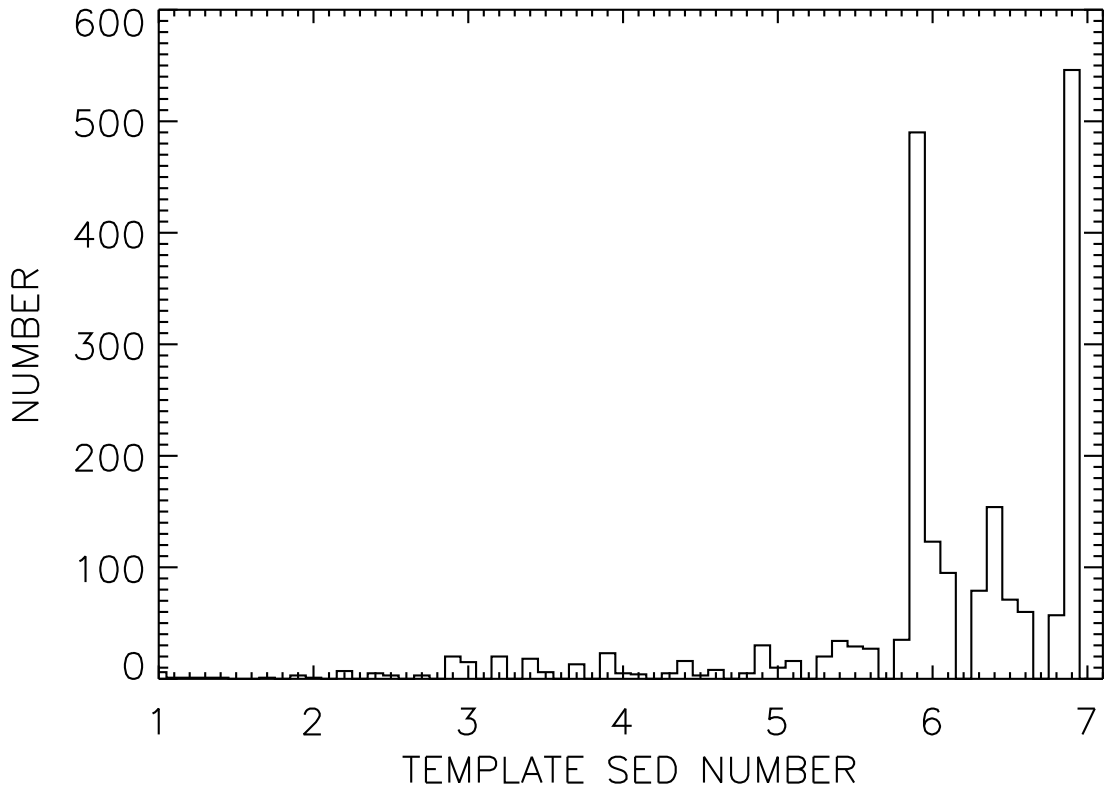
Fig. 2.— The histogram of SED template numbers for all sources with redshifts greater than 2.0. The interpolated templates go in increments of 0.1 between the primary template SEDs.
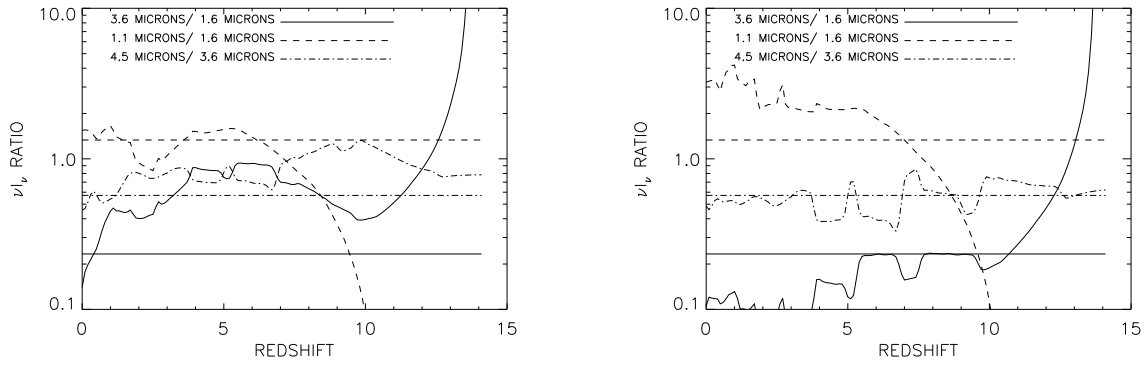
Fig. 3.— The predicted ratios of the powers, νI_ν, in the F110W band to the F160W band, dashed line; the the 3.6μm *Spitzer* band to F160W band, solid line; and the *Spitzer* 4.5μm to 3.6μm band, dash dot line; versus redshift. The straight horizontal lines indicate the observed values of the ratios at an angular scale of 100″ with the same line style code. a) (left) is for template6 and b) (right) is for template 7, the hottest SED, which is consistent with a possible Population III galaxy.
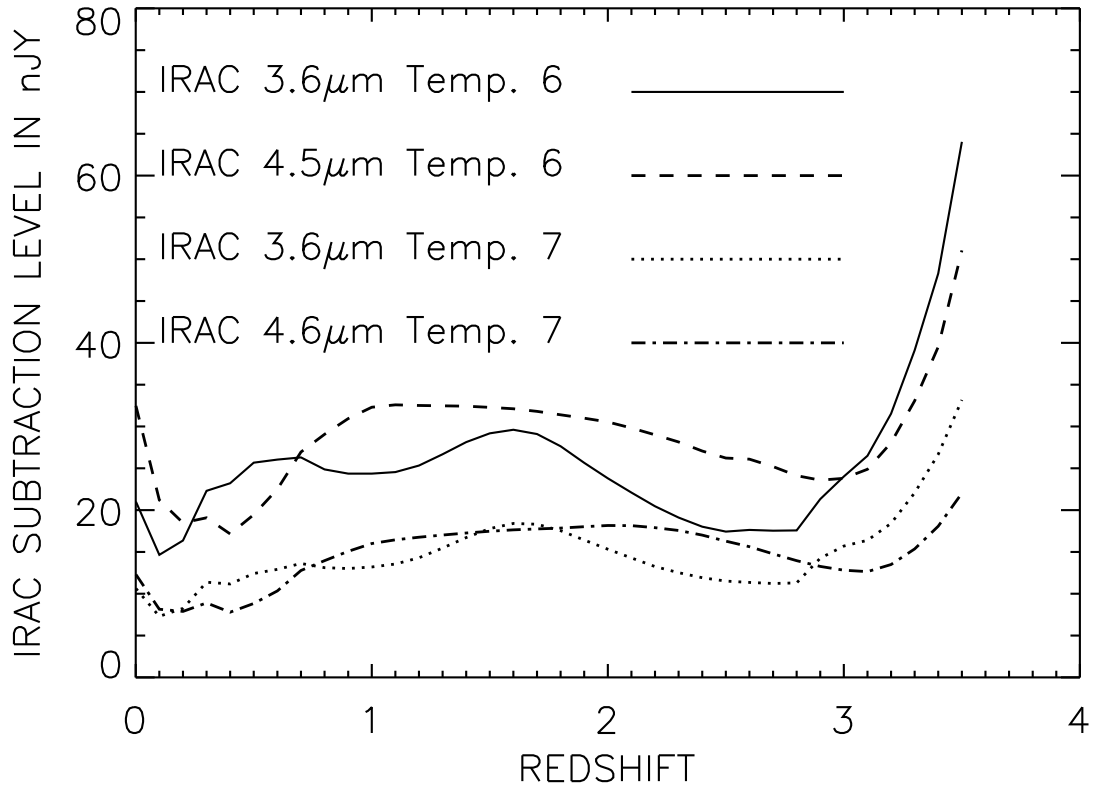
Fig. 4.— The figure shows the IRAC fluxes in the 3.6μm and 4.5μm bands that correspond to a subtraction limit of 3.7 nJy in the ACS F775W band as a function of wavelength for the two templates (6 and 7) used in this study. The quoted subtraction level from Kashlinsky et al. (2007b) is 10 to 20 nJy, consistent with subtraction levels in the figure. The sharp rise at approximately z=3 is when the Lyman break starts to enter the F775W band.
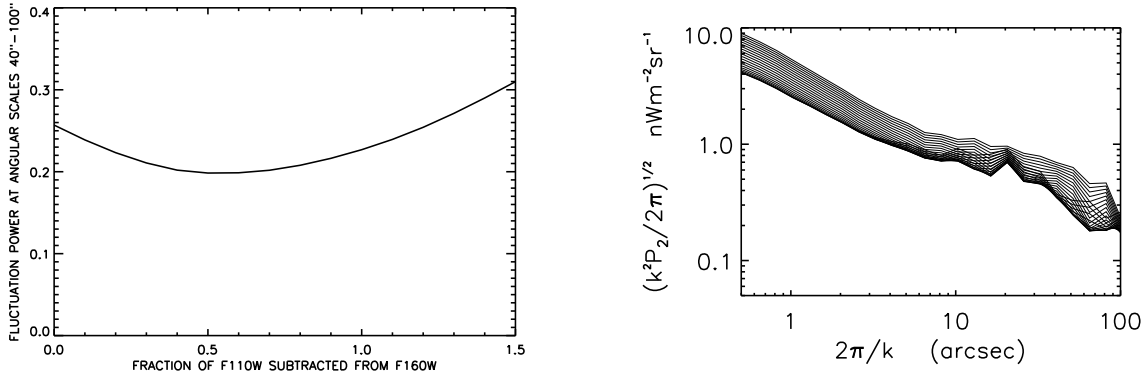
Fig. 5.— a) The left panels shows the $\ln(k)$ weighted sum of fluctuation power for angular scales greater than $30''$ versus the scaling factor of the F110W image subtracted from the F160W image. The minimum is at a scaling factor of 0.6. b) The right panel shows the nested fluctuation power spectra for the different scaling factors. The lower boundary is the limit for the contribution of high redshift sources plus other sources of spatial noise.

Table 1.   Properties of the template SEDs. Both SEDs are taken from models of Bruzual & Charlot (2003) based on the Padova 1994 models. The IMFs are from Chabrier (2003).

Template Number	Metallicity	IMF	Low Mass Limit	Upper Mass Limit
6	0.004	Chabrier	0.1	100
7	0.0001	Chabrier	0.1	100